After-coal diamonds: an enigmatic type of impact diamonds

Tatyana G. Shumilova[1,2*], Sergey I. Isaenko[1], Vasily V. Ulyashev[1], Valery A. Kazakov[3], Boris A. Makeev[1]

[1]Institute of Geology, Komi Scientific Center of Ural Division of Russian Academy of Sciences, Pervomayskaya st. 54, Syktyvkar, 167982, Russia

E-mail: shumilova@geo.komisc.ru

[2]Hawaii Institute of Geophysics and Planetology, University of Hawaii at Manoa, 1680 East-West Road, Honolulu, HI, 96822, USA

[3]SSC FSUE Keldysh Research Centre, Onezhskaya, 8, 125438, Moscow, Russia;

E-mail: nanocentre@kerc.msk.ru

Abstract

Impact diamonds were discovered in the 70s and usually accepted as being paramorphs after graphite, resulting in grains of extremely high mechanical quality. A diffusion-less mechanism for the graphite-to-diamond transition under huge pressure has been experimentally realized and theoretically explained. Besides, another type of impact product has received much less attention, namely diamonds formed after coal as a result of the impact. Here we describe after-coal impact diamonds from the giant Kara astrobleme (Pay-Khoy, Russia), which resulted from a large asteroid impact about 70 Ma ago. The impact created a large number of unusual impact diamonds, which are described here for the first time using high-resolution techniques including visible and UV Raman spectroscopy, scanning electron microscopy (SEM), atomic force microscopy (AFM) and transmission electron microscopy (TEM). Two main varieties of after-coal diamonds occur: micrograined (sugar-like, subdivided into coherent and friable) and, as a new type, paramorphs after organic relics. After-coal diamonds differ from after-graphite impact diamonds by the texture, the absence of lonsdaleite, a micro- and nanoporous structure.

The sugar-like variety is presented by tightly aggregated well-shaped single nanocrystals. The after-organic diamond paramorphs are characterized by a perfect-preserved relict organic morphology, sub-nanocrystalline–amorphous sp^3-carbon (ta-C) nanocomposites and specific properties. Based on the description of after-coal diamonds, we propose a new, polystage formation mechanism: high-velocity coal pyrolysis with hetero-elements removal followed by pure carbon crystallization with local diffusion process resulting diffusion-limited crystallization. Also we propose similarity of the aftercoal diamonds features to carbonado.

Key-words: astrobleme, impact diamond, coal, diamond paramorphs, after-coal transformation, carbon, carbonado, shock metamorphism.

1. Introduction

Impact diamonds have been attracting significant attention since their initial discovery. There are numerous publications devoted both to their formation mechanisms and to the formation of the related impact craters (Bundy & Kasper, 1967; Masaitis et al., 1972, 1990, 1999; Sokhor et al., 1973; Shafranovsky, 1985; Val`ter et al., 1992; Decarli, 1995; Langenhorst et al., 1998; El Goresy et al., 2001, 2003; Langenhorst, 2002; Vishnevsky, 2007; Kvasnytsya & Wirth, 2013; Smith & Godard, 2009; Ohfuji et al., 2015). Impact diamonds display exceptional mechanical properties such as extreme hardness and can occur in large deposits with high concentrations, such as in the Popigai astrobleme (Masaitis et al., 1972, 1990, 1999). It is usually accepted that impact-diamond formation is the result of a solid-state transformation (diffusion-less process) of graphite to diamond at high pressures (≥ 30 GPa). This transformation process has been supported by experimental and theoretical studies (*e.g*. Lonsdale, 1971; Kurdumov et al., 2012; Xie et al., 2014). Diamond production under shock pressure is known to be also possible from differently ordered carbons and coal, through a diffusion-limited reconstructive mechanism (Borimchuck et al., 1991). However, the detailed mechanism of diamond formation

from coal is completely unclear. Besides, experiments using Kara sedimentary organic material as precursor (Korochantsev, 2004) suggest that the shock pressure for the bituminoid-to-diamond transformation has to be essentially higher than that for the graphite-to-diamond transition. Indeed, in the experimental study of such a transformation, diamonds were not produced from bituminoid even under 60 GPa, only nanocrystalline graphite was formed (Martirosyan, 2014).

Although impact after-coal diamond products are known from nature, information about the natural transformation of non-graphitic carbon to diamond is scarce. A few detailed studies devoted to such type of impact diamond and their occurrence are related to the Kara astrobleme (Yezerskiy, 1982, 1986; Mashchak, 1990, 1991; Shishkin et al., 2012). The Kara astrobleme (about 65 km in diameter) resulted from the impact of a large asteroid about 70 Ma ago (Masaitis, 1975; Nazarov et al., 1989, 1990, 1991, 1992; Koeberl et al., 1990; Kolesnikov et al., 1990; Mashchak, 1990, 1991; Trieloff, 1998; Shishkin et al., 2012) and is the only known astrobleme in the northeastern European part of Russia that has been described as containing diamonds formed essentially from coal rather than from graphite (Yezerskiy, 1986). According to recent data (Shishkin et al., 2012), the prospected resources of impact diamond in the Kara astrobleme are 200 kg/km^2.

Here we characterize for the first time a variety of after-coal carbon phases from the Kara structure by detailed nanostructural analysis using high-resolution methods, including visible and ultra-violet Raman spectroscopy, scanning electron microscopy (SEM), atomic force microscopy (AFM) and transmission electron microscopy (TEM). The observations reveal unusual nanostructural features and suggest a specific mechanism of Kara diamond formation.

2. Kara astrobleme target composition

2.1. Geological setting

The twin impact craters Kara and Ust`-Kara are located in the northeastern European part of Russia belonging to the northeastern section of the Pay-Khoy Ridge structure (Fig. 1). The

craters have diameters of 65 and 25 km, respectively. The Kara astrobleme is fully on land while Ust`-Kara partly extends just beyond the coastline of the Kara Sea, and is generally under water at present. The Kara astrobleme is obvious today as a depression in the landscape, and is well expressed in gravitational- and magnetic-field surveys (Mashchak, 1990, 1991; Shishkin et al., 2012).

Past studies on the origin of the Kara astrobleme have been controversial. Until the 1970s, the origin of the Kara depression was assigned to a volcanic eruption. In 1970, P.S. Voronov wrote in a media press about the impact hypothesis, which was immediately supported by V.L. Masaitis in 1971 and further developed by industrial geologists headed by M.A. Maslov and G.Ya. Ponomarev (Mashchak, 1990, 1991). Subsequent scientific studies have been carried out since the 1980s by, *e.g.*, Yushkin & Lysyuk (2001) and Mal`kov & Andreichev (2010). Most recently, the full range of silica polymorphs, including high-pressure coesite and low-pressure post-impact phases, was described in Kara impactites by Lutoev & Lysyuk (2015).

The Ust`-Kara astrobleme has been known since 1976, when its nature as an independent impact crater, of contemporary origin with the Kara astrobleme, was determined (Mashchak 1990, 1991). At present it is accepted that the Kara and Ust`-Kara astroblemes resulted from the same impact event produced by a single bolide that broke up before contact with the Earth's surface.

2.2. Geological composition of the sedimentary target

The geological composition is described here after Mashchak (1990) and Shishkin et al. (2012), who studied the region in detail and ascribed the Kara region to the Pay-Khoy subzone of the Zilairo-Lemvinskaya zone on the basis of the bathyal sediments present in the Sylovayachinskaya (D_3–C_1), Karskaya (C_1) and Karasilovaya (C_2–P_1) units.

According to these authors, the target in the Kara and Ust`-Kara astroblemes region consists of two structural levels – Late Proterozoic (bottom) and Paleozoic (upper) sediments

(Fig. 1). The upper structural level consists of Ordovician-Carboniferous and early Permian sediments. The lower one consists of mica-clay, siliceous and actinolite-bearing phyllites with lenses of metamorphosed rhyolites and tuffs, with a total thickness of more than 6 km. At the center of the Kara astrobleme these lithologies occur at a depth of about 500 m. The rocks are folded as in the Pay-Khoy anticlinorium system.

The upper structural level is comprised of two subunits. The bottom sublevel consists of about 3.5 km thick Ordovician-Carboniferous sediments, where the Ordovician sediments consist of clay-siliceous, mica-siliceous and carbonate-clay shales, clay and mica-containing limestones measuring 1.2-1.5 km in thickness. The $S–D_1$ sediments are undivided, have a thickness of about 370 m, and consist of black coal-clay, coal-siliceous, coal-carbonate-siliceous and graphitic-siliceous shales with sublayers of quartz-containing limestones. The $D_2–D_3$ sediments of 700–900 m total thickness are pure or carbonate-containing sandstones, coal-siliceous, siliceous and clay shales, jasperoids, dolomitised and marmorised limestones. The Carboniferous system has a total thickness about 760 m. It is composed mainly of coal-clay, coal-siliceous and clay-siliceous shales, of coal-, clay- and silica-containing limestone for the bottom level (C_1 sediments). The Middle and Upper Carboniferous rocks are made up of 170 m thick coal-siliceous and chlorite–sericite siliceous shales. Both Devonian and Carboniferous sediments are intensely fragmented.

The upper sublevel is represented by structurally discordant early Permian sediments with a maximum thickness of 2.1 km, widely distributed in the north-eastern part of the Pay-Khoy Ridge. It is characterized by polymict sandstones, siltstones, sandstones, clay shales with sublayers of limestones, coals and conglomerates, reaching a thickness of up to 2 km. This structural level is less deformed than the bottom sublevel, and shows simple folding.

The Paleozoic sediments are overlain by Pliocene-Quaternary sediments with a typical thickness of 5–10 m, rarely up to 60 m, which widely cover the area including the Kara astrobleme region.

It is clear from this lithological description that the Kara target contains a significant quantity of coal-containing sediments, amounting to hundreds of meters in thickness. This is the most important feature of the giant astrobleme, in which the carbonaceous matter was the source of carbon that resulted in diamond formation during the giant Kara impact event. This event occurred around the Cretaceous–Paleogene boundary, with the estimated age ranging from 55 to72 Ma depending on the methods used (*e.g*. Mashchak, 1990, 1991; Mal`kov & Andreichev, 2010). According to the most recent ^{40}Ar-^{39}Ar determination on impact-melt rocks, the age corresponds to 70.3 ± 2.2 Ma (2σ) (Trieloff et al., 1998).

2.3. Impact rocks of the Kara astrobleme

According to Shishkin et al. (2012), a specific Kara complex of rocks connected to the impact event (impactites) can be divided into three units, including (from bottom to top) allogenic lithic breccias, suevites, and tagamites, depending on the proportion of melt (impact glass/crystallized impact melt) in the brecciated rocks (<15, 15–65 and >65 vol%, respectively). Here we provide a brief description of the impact units after Machshak (1990) and Shishkin et al. (2012).

The *allogenic lithic breccias* are characterized by dislocated impact-metamorphosed rocks of the target and are composed of gigabreccia (fragments size from 10–50 m up to 300–500 m), megabreccia (1–10 m) and block breccia (0.2–1.0 m) with wide distribution of shatter cones. The entire unit is 0.7–0.9 km thick at the crater center.

Suevites occur as a 0.8–1.0 km thick unit that covers the allogenic breccias and locally the Paleozoic sediments. The size of the breccia fragments increases toward the bottom of the unit, they consist mostly of litho-clasts (up to 85% among the fragments). Suevites occur as lappile-agglomerated, agglomerated, and rarely as block vitro-clastic types. The latter is characterized by 15–30 vol% of “glass” with isometric, elongated and irregular shapes from small drops up to meter-sized bodies with spot-like, striped and fluidal texture. Litho-clasts within the “glasses”

can be fully melted or just preserved as blurred objects. Lapille and lapille-agglomerated litho-vitro-clastic sintered suevites are very rare, and consist of unsorted clastic material with 50–80% "glass" and 20–50% litho-clasts.

Tagamites are locally spread, mostly in the basin of the Anaroga river, forming lava-like bodies; they occur as lens and layer-like bodies with complicated shapes up to 15 m thick with up to 200–300 m horizontal extension. They consist of "glasses" with a total loss of the host sediment texture. Tagamites have essentially a lower content of clastic rock- or mineral fragments, ranging from 5 to 35 vol% of the whole rock. They have lens-spot, spot-fluidal textures, resulting from different levels of crystallization.

2.4. Target carbonaceous matter characterization

According to Yudovich et al. (1990), the carbonaceous matter of the Pay-Khoy is mostly either finely dispersed in black shales or occurs in concentrated form in coal layers with a thickness of about 10 cm. Besides, our own field observations revealed that the coal layers within the target area could be at least up to 2 m thick (Fig. 2d). This finding is based on the presence of quite large coal fragments within suevites that are exposed at the surface, where they are intensely weathered and disaggregated.

In coeval black shales from the southern part of the Pay-Khoy Ridge, containing from 1 up to several wt% C_{org}, Yudovich et al. (1990) report low bitumen content and high concentrations of aromatic rings in the carbonaceous matter. The largest C concentration was measured at about 30 wt% for Late Devonian clay-siliceous shales. Transmission electron microscopy (TEM) data of the carbonaceous matter revealed globular-like aggregates made of small globules 6 nm in diameter, with the diffraction patterns having 3.37 Å *d*-spacings and wide rings with 2.02 and 1.17 Å *d*-spacings. The exothermal oxidation effect (in differential thermo-gravimetric analysis, DTG) for the carbonaceous matter started between 500–600°C with double maxima in some cases. Thus, Yudovich et al. (1990) have described the matter as comprised of two differently

ordered carbon types – an amorphous/shungite-like carbon and a turbostratic graphite ~~carbon~~. The first type was assigned a bathyal sedimentary origin, having an autochthonous nature, whereas the graphitic matter (turbostratic graphite) was considered to be para-autochthonous, resulting from a migration process.

2.5. Previous work on Kara impact carbons

In previous studies (Yezerskiy, 1982, 1986; Reshetnyak & Yezerskiy, 1990), after-coal impact carbons were studied only for size fractions larger than 0.5 mm. Yezerskiy (1986) described several varieties of after-coal carbons chemically extracted from Kara astrobleme impactites. He described them as irregularly shaped fragments with sizes up to 1.6 mm, sometimes rounded grains, many of which had an optically visible friable and porous structure. Some grains had a hard covering but were empty inside. Some carbon particles occurred as optically transparent amber-like fragments, while others were opaque with black, gray, brownish, light blue or white color. Among them, the dense particles were harder than moissanite, and the porous varieties could be easily broken. Three types of carbonaceous grains were described on the basis of color – A, B and C (Table 1), which occur as independent particles or as aggregates consisting of different varieties and with gradual transitions between them. The phase-state determination of the individual carbons was made on the basis of Laue X-ray studies.

Variety A, with black color, was described by V.A. Yezerskiy as an intermediate state between coal and diamond. Varieties B and C were identified as diamonds, where B occurred as brown grains (subvariety B_1) and aggregates of brownish, white and blue layers (subvariety B_2). Variety C was categorized as white grains, with a texture recognized by optical observations and Laue X-ray studies. This variety might occasionally contain lonsdaleite (Yezerskiy, 1986).

In the following, on the basis of high-resolution techniques, we describe the most important carbon phases (Table 1, Figs. 3–9) that are reliably characterized for the impact-rock fractions with sizes <2 mm, including the diamond size fraction <0.5 mm. Attention is paid to

the description of the after-coal diamonds. In addition, other carbon phases that are syn-genetic to diamonds within the studied impact rocks, including abundant glass-like carbon and rare impact graphite, are described here briefly but are subjects for future, more detailed studies. Our classification of Kara impact carbons is based on structural state and morphology; the correspondence with earlier categorizations (Yezerskiy, 1986) and some general characteristics of carbons are given in Table 1.

3. Material and methods

Studied material. The material was sampled in 2015 by the Russian team during a field expedition to the southern part of the Kara astrobleme, covering the region of the Anaroga, Kara, Sopcha-Yu and Sibirchata-Yacha river basins. We focus here on material from the regions of the Anaroga and Kara rivers. The study combines preliminary standard mineralogical, petrological, and geochemical investigations with a detailed mineralogical study of carbon phases using high-resolution methods for separated particles and *in situ* inclusions in rocks.

For *in situ* studies we have prepared fresh mechanically crushed surfaces and polished thin sections for studies in transmitted and reflected light and for instrumental measurements. Non-diamond-containing materials such as Cr_2O_3 and Sr_2O were used for polishing. Preliminary epoxy impregnation of the suevites was prepared, without the use of any covering glass and balsam covering of the thin sections. For the studies of the carbonaceous matter many measurements were carried out with control of fresh crushed rock surfaces and extracted grains in order to avoid the possibility of contamination by epoxy glue.

The carbon phases were extracted from the host impact rocks at the Laboratory of Diamond Mineralogy at the Institute of Geology of Komi Scientific Center of Russian Academy of Sciences (IG Komi SC UB RAS, Syktyvkar, Russia) using the thermochemical dissolution technique used for microdiamond concentration. The technology allows enriching

239 microdiamonds with sizes >1 μm; it includes a complex multiple-stage chemical treatment such
240 as boiling in a mixture of concentrated H_2SO_4 and $K_2Cr_2O_7$ aqueous solution, melting with
241 NaOH at 500°C, treatment by HCl aqueous solution. We used small-volume dissolution with an
242 initial rock mass of 5 g per sample. The concentrated particles were picked up from the filters
243 under an optical binocular microscope MBS-10 at magnification ×40, and then were studied in
244 detail by the methods described below.

245 *Optical observations* were made using Polam 312 and Olympus BX41 microscopes in
246 transmitted and reflected plane- and cross-polarized light with objectives ×4.7–100 (IG Komi SC
247 UB RAS, Syktyvkar, Russia).

248 *Raman spectroscopy* analysis was performed at IG Komi SC UB RAS using a high-
249 resolution Raman spectrometer LabRam HR800 (Horiba Jobin Yvon, France). Spectra were
250 collected *in situ* from surfaces of fresh crushed impact rocks, polished thin sections, and from
251 individual chemically concentrated grains. An Ar^+ excitation laser with 488-nm wavelength was
252 used to collect spectra in the range 100–8000 cm^{-1} at room temperature, with 1.2 mW laser
253 power. The use of ×50 and ×100 objectives and a grating with 1800 groves/mm yielded
254 approximately 1-μm spatial and 1-cm^{-1} spectral resolutions.

255 An experimental treatment aimed at recovering diamond from grains coated by glass-like
256 carbon was applied by *in situ* laser combustion of the coating. In such case the laser power was
257 raised until the outer glass-like cover was burnt and the diamond core appeared. Usually the final
258 laser power output for combustion experiments was no more than 12 mW, but reached 72 mW in
259 some cases. The diamond phase was confirmed by Raman spectra (T_{2g} scattering mode) and
260 optical observations.

261 To ascertain the diamond nature of the after-coal diamonds, ultraviolet (UV) Raman
262 spectroscopy studies were performed at the SSC FSUE Keldysh Research Centre (Moscow,
263 Russia) with a T64000 (Horiba Jobin Yvon, Japan) Raman spectrometer using a 244 nm laser
264 excitation wavelength with a grating of 2400 grooves/mm, and a 40× objective. To prevent laser-

induced sample damage, the laser power on the sample was decreased to ~5 mW power, while a laser spot diameter ~5 μm and an exposure time of 5 min was used.

All spectra were checked by pre- and post-observations with an optical microscope to check for possible specimen changes after laser exposure. After background correction, all spectra were deconvoluted to individual peaks using a curve fitting procedure by Gaussian and Lorentzian functions from the software provided by LabSpec 5.36.

Scanning electron microscopy and microprobe analysis (EMP). Analysis of the impact rocks and carbonaceous matter was made at the IG Komi SC UB RAS with *in situ* observations in fresh rock surfaces and carbon-grain concentrates using a VEGA 3 TESCAN scanning electron microscope (Tescan, Czech Republic) with a VEGA 3LMN, INCA ENERGY 450 energy-dispersive detector that was used for mineral chemical and morphological analysis. The measurements of elemental contents were done without any conductive covering to avoid analysis contamination when analyzing carbon *in situ*. Afterward, the diamond specimens were covered by a conductive thin carbon film for high-quality SEM images.

Atomic force microscopy. An atomic force microscope Integra Prima (NT-MDT, Russia) was utilized to study fresh surface morphology. Silicon cantilevers with 25 nm-thick conducting Pt coating and 20 nm tip radius (PPP-CONTPt, Nanoworld) were employed at room temperature (25–27 ºC) and about 65% relative humidity. The diamond grains were set on electrical conducting glue without any conducting covering. The average nanocrystallite sizes were calculated with statistical analysis of the morphological nanoimages.

Transmission electron microscopy. The preliminary TEM studies were conducted at the IG Komi SC UB RAS with powder specimens of the carbon particles concentrates using a Tesla BS 500 (Czech Republic) TEM at 60 kV accelerating voltage. Specimens were prepared by ultrasonic suspension in ethanol and crushing of individual diamond grains with settling on a holey carbon supporting film.

4. Description of the host-rocks

Here we briefly describe the features of the Kara impact rocks – host tagamites and suevites containing after-coal diamonds and associated carbons – sampled by our team in the Anaroga and Kara regions.

4.1. Tagamite

Tagamite was sampled at the Anagoga River from a large layer-like body with a maximum visible thickness of 7–8 m (Fig. 2a), with occasional inclusions of large coal fragments at the bottom of the body (Fig. 2b) and microsized fragments within the melt rock matrix (Fig. 2a, inset). Tagamite has light brown color, massive texture with fluidal rock structure mostly comprised by "glass" - solidified partly crystallized impact melt (up to 80–90 vol%) with rare relics of the target rocks such as sandstones, minerals and coals (Fig. 2a, b, insets).

The rock clasts in tagamite have rounded edges, but the shape of the initial clast may be recognized as a melt-treated outter zone. The relict clasts are generally pieces of sandstones with sizes up to 8–10 cm, and rarely shales or minerals. The tagamite "glass" is ~~essentially~~ slightly altered due to the ~70 m.y. elapsed since the impact event. The "glass" appears opaque, as a crypto-crystalline gray-brown, quite soft matter, which easily disaggregates during drying at room conditions. It contains less than 1 wt% of carbonaceous matter, according to DTG analysis. The "glass" generally consists of a cryptocrystalline alumino-silicate substance represented mainly by albite according to X-ray diffraction and Raman spectroscopy. The specific feature of the tagamite matter is the essential presence of molecular water in a chemically unbound state. A true glass, either in tagamites or in suevites, is characterized generally by aluminosilica and SiO_2 and was rarely found, mainly as thin rims surrounding pores within the rock. According to our field observations and petrochemical studies, we assume that tagamites were formed after target sandstones, consistent with the earlier studies of Selivanovskaya et al. (1990).

4.2. Suevites

317 *4.2.1. The suevites syngenetic to tagamites*

318 The suevites syngenetic to tagamites (Fig. 2a) are represented by layer-like lens bodies
319 with a visible maximum thickness of 6–7 m. They have a macroscopically obvious breccia-like
320 structure with variable content of the target fragments consisting mainly of sandstones and
321 siltstones, making up to 50-60 vol% of the total rock. The suevites have brownish color similar
322 to the tagamites and show a transition to tagamites. The "glass" is well recognized within the
323 suevites by their fluidal texture (Fig. 2a, inset), it preserves some relics of coal fragments. After
324 dissolution we have found that a 5-g standard sample of tagamite and connected suevite includes
325 at least 5–10 diamond grains with sizes up to around 50–100 μm.

326 4.2.2. *The suevites unconnected to tagamites*

327 Suevite sampled on the right bank of the Kara River is essentially different from that
328 described above. It has gray color and an essentially porous structure with a lot of micro- and
329 macrogeodes filled by calcite and quartz. The suevite matrix consists predominantly of
330 carbonate, and the breccia fragments are comprised of black shales, limestones and coal
331 fragments (Fig. 2c). The coal fragments can reach 2 m in size (Fig. 2 d). At the same time some
332 quite large sandstone fragments and light-colored "glass" occur within the suevite, reaching
333 several decimeters in thickness and >1 m in length.

334 According to our field observations and microscopic studies, we assume that the Kara
335 suevite was formed from carbonate sediments, black shales and some part of coal layers of the
336 target. For a detailed study, part of a "glass" lens-like body about 1.5 m long and 15 cm thick
337 was dissolved for diamond recovery. As a result it was estimated that every 5 g of the "glass"
338 included at least five fully crystalline diamond grains up to 100–200 μm in size, as well as up to
339 200–300 diamonds in the form of after-organic paramorphs with a similar particle-size range. On
340 the basis of the number of extracted grains, the after-coal diamond concentrations can be
341 expressed to a standard diamond unit: up to 85 carat per ton for the impact rock, and up to 3000
342 carat per ton in the solidified impact melt.

5. Results: impact carbons

5.1. Diamonds

Kara after-coal diamonds extracted from chemical concentrates occur as polycrystalline grains up to 200 μm in size (Fig. 3–5). On the basis of morphological features we have divided them into two main varieties of after-coal diamonds – micrograined (sugar-like, subdivided into coherent and friable) and paramorphs after organic relics. Here we describe the mineralogical features of the after-coal diamonds; their technological properties will be addressed elsewhere.

5.1.1. "Sugar-like" diamonds

The diamonds occur mainly in irregular shapes, mostly with rounded edges up to wholly rounded forms (Fig. 4a-c). Rarely they have a layered texture and morphology preserved after organic relics (Fig. 4f). This diamond type occurs at about 85 carats per ton in the studied impact rocks. Although they are usually white in color, they can also have gray and slightly gray, sometimes gray-blue and brownish shades. They generally have optically recognizable micrograined "sugar-like" surfaces without optically noticeable "diamond" luster, and only rarely have smooth surfaces with a medium greasy luster. We call these diamonds "coherent sugar-like diamond".

Raman studies with visible laser excitation (Fig. 6, left column) over a wide spectral range show that the "coherent sugary" diamonds are characterized by numerous luminescence bands on the basis of high total luminescence intensity. In Raman spectra obtained with UV laser excitation the diamond band corresponding to T_{2g} stretching is at the standard position of 1332 cm^{-1}, with a full-width at half maximum (FWHM) of about 10–30 cm^{-1} (Fig. 7). In spectra taken using visible laser excitation, a band around 1600 cm^{-1} belongs to a G-band of sp^2-carbon; the features at 1450-1475 and 1710 cm^{-1} are observed as luminescence bands.

Among the light-colored diamond varieties with different shades of color, there are numerous “friable sugar-like diamonds” that occur as opaque, irregularly shaped polycrystalline grains without rounded edges grains nor bright luster. With visible laser excitation they have an unrecognizable diamond Raman band concealed by an intense luminescence (Fig. 6, spectra 2–4). The UV Raman spectra demonstrate that the white friable opaque carbon micrograins are indeed polycrystalline diamonds (Fig. 7).

5.1.2. After-organics diamond paramorphs

In our study brown diamonds are characterized as optically transparent matter having surfaces with bright lustre that occur mostly as paramorphs after organics, preserving relict morphology of the initial organic matter as shown by optical microscopy or SEM (Fig. 3 b-d, 4 i-l). They occur in tagamite and suevite samples, in impact “glass” and are accompanied by impact “sugar-like” diamond and glass-like carbon. In impact “glass” the brown diamonds are very abundant, comprising up to a half of the carbon particles within a chemical concentrate, yielding up to 200–300 particles per 5 g sample of a “glass” from suevite (up to several thousand carat per ton, as noted above).

In transmitted cross-polarized light the diamond is anisotropic without optical extinction. Due to a very high luminescence background, the diamond Raman band at 1332 cm^{-1} is usually concealed when excited by the visible laser (Fig. 6, spectra 3, 4), which does not allow a standard phase-state analysis. However, in some cases the diamond line can be recognized in the brown carbon despite the high luminescence (Fig. 6, spectrum 4). For all studied cases the comparison of white and brown diamond luminescence allowed observing similar band features.

The UV Raman measurements were the most useful for phase determinations, and clearly demonstrated the diamond nature of the after-organic diamond paramorphs (Fig. 6, right column). However, this diamond type shows a large downshift of the diamond band (1317–1326 cm^{-1}) relative to the standard value of 1332 cm^{-1} (Fig. 7), and also shows a wide associated

FWHM of about 40–60 cm^{-1}, which is usual in nanocrystalline diamond (Yoshikawa et al., 1993, 1995; Prawer, 2000; Ferrari, 2004; Piscanec et al., 2005; Vul`, 2006; May et al., 2008; Osswald et al., 2009). The downshift due to heating is larger for nanosized material than for regular-sized one (May et al., 2008; Isaenko & Shumilova, 2008).

Debye-Scherrer X-ray analysis supports the identification of the brown after-organics paramorphs as diamond. The X-ray pattern shows a single small-intensity ring, without any hint of spots at all, corresponding to polycrystalline diamond with a spacing d_{111} = 2.05 Å. Electron diffraction patterns of the brown diamonds are characterized by three rings corresponding to (111), (220) and (311) planes of cubic diamond (Fig. 5a). No texture was recognized by electron diffraction. Preliminary tests of the mechanical properties show high fragility of after-organics diamond paramorphs and very high hardness of their crushed fragments.

5.1.3. Kara diamonds nanostructure

Here we describe the results of our comparative study of white coherent sugar-like and brown after-organics diamonds (Fig. 8), which were selected for a detailed analysis by atomic force microscopy (AFM) as they have essentially different morphological and spectroscopic features. According to AFM observations all impact after-coal diamonds occur as nanopolycrystalline aggregates with different degrees of crystallinity, varieties of shapes, and sizes of nanocrystals (Fig. 8).

The white “sugary” diamonds (Fig. 8 a, b) are characterized by aggregates of 20–40 nm nanocrystallites tightly joined together into larger units reaching 80–100 nm in size, or forming continuous aggregates.

The after-organics diamond paramorphs are quite diverse in their crystallinity (Fig. 8 c–f). In a first case they are characterized by poorly distinguishable nanocrystallites, from a few tens of nanometers up to 150 nm in size (Fig. 8 e, f). Another case of after-organics diamond contains

small octahedral nanocrystallites with an average size about 140 nm that are distributed more uniformly through the nanopolycrystalline aggregate (Fig. 8 c, d).

All the recognized Kara-impact after-coal diamond types are characterized by quite a rough surface at the nano-scale, with deeply porous structures and an almost complete absence of carbon cement between the crystallites. The AFM results are consistent with TEM observations and electron-diffraction data in showing that the Kara after-coal diamonds occur as polycrystalline diamond grains devoid of any layered texture in the aggregates (Fig. 5a).

5.2. Graphite

Novel, quite rare graphite particles formed under impact process have been recognized in suevites connected to tagamites. The graphite occurs as polycrystalline aggregates (Fig. 3 e, f) with sizes up to several hundred micrometers, or as individual micro- and nano-particles revealed by TEM and Raman spectroscopy. The particles usually have irregular shapes with a flattened morphology for individual grains. The polycrystalline nature of graphite particles has been established by optical microscopy (Fig. 3 e, f), electron diffraction (Fig. 5b) and Raman spectroscopy (Fig. 6, spectrum 6) on the basis of relative intensity of the D band and FWHM of the G band of sp^2 carbon, which are inversely proportional to the graphite crystallite size (Tuinstra & Koenig, 1970; Wopenka & Pasteris, 1993; Ferrari & Robertson, 2004). The first-order region of the Raman graphite spectrum (Fig. 6, spectrum 6) consists of a strong and narrow 1581 cm^{-1} line of the E_{2g} graphite mode with a FWHM of 26 cm^{-1} which corresponds to ~ 10–30 nm crystallite sizes. The 1358 cm^{-1} band belongs to a disordered feature of graphitic carbon, named the D-band. The second graphite order is present in the spectrum with the 2441, 2741, 2949 and 3245 cm^{-1} bands.

5.3. Glass-like carbon

Glass-like carbon (GLC) is the most abundant impact carbon phase. It occurs in black grains with sizes up to several hundred micrometers with irregular shapes as breccia-like micro-fragments. They have glassy surfaces with bright reflection and, much more rarely, occur as paramorphs after organic matter similar to the described diamond grains (Fig. 4c, 4 i-l). The phase state of the glassy carbon variety was characterized by high-resolution Raman spectroscopy (Fig. 6, spectrum 5). The bands at 1359 and 1598 cm^{-1} correspond to D and G bands of sp^2 carbon, the bands in the region 2400–3300 cm^{-1} belong to a second order of the graphitic carbon. These spectroscopic features are in a good correspondence with industrially produced glass-like carbon (Harris, 1997).

5.4. After-coal diamonds with GLC coats

Among products recovered by chemical dissolution, special attention was devoted to diamonds coated by glass-like carbon. They look like usual GLC fragments with irregular morphology and bright reflectance, yet at the same time they are denser than usual GLC. During detailed *in situ* Raman studies the diamonds were exposed by intense laser heating directly under the microscope, as explained in the Procedure section. Thus, after burning the GLC covering, a diamond core could be exposed and became visible by optical microscopy, with the corresponding appearance of the Raman diamond band at 1318-1321 cm^{-1} (Fig. 9), downshifted due to overheating by the laser heavy treatment (May et al., 2008; Isaenko & Shumilova, 2011). The same results were produced by several similar experiments to prove the burning of the GLC coating and exclude GLC-to-diamond transition under laser treatment.

6. Discussion

6.1. The status of “togorite”

Based on the observations of this study we have distinguished among the proven after-coal impact carbons: glass-like carbon, diamond (two varieties with two subvarieties), and graphite (Table 1). The typomorphic features of diamonds coated by GLC demonstrate that they are similar to the previously described "togorite" (Yezerskiy, 1982; variety A in Yezerskiy, 1986), proposed as a new carbon mineral (non approved by the IMA). The aggregates comprised of diamond (core) and glass-like carbon (coat) should provide macroscopically high hardness and density in accord with the relative proportions of diamond and GLC components. We therefore conclude that the intermediate state between diamond and coal named "togorite" by Yeserskiy (1982) is just diamond coated by GLC, and so does not represent an independent carbon phase.

6.2. After-coal diamond features, after-organic diamond paramorphs

Among the recognized after-coal diamonds, we have categorized two varieties that essentially differ from after-graphite impact diamonds: (i) *sugar-like* fully crystalline-ordered nanocrystalline aggregates *with coherent and friable subvarieties*; (ii) *after-organic paramorphs*, consisting in nanocrystalline–sub-nanocrystalline–ta-C aggregates with various proportions of crystalline and amorphous carbon. The varieties are well distinguished between them by a complex data and differ from the earlier published data on after-coal diamonds (Yezerskiy, 1986; Reshetnyak & Yezerskiy, 1990) (Table 1, Fig. 7).

The after-organics diamond paramorphs have been found for the first time. These grains have specific typomorphic features that differentiate them from the other after-coal diamonds – morphology, optical transparence, brown color, very high luminescence, spectral features, nanocrystalline state, ordering level. Considering the well-preserved morphology of organics one may assume that the diamond paramorphs were formed directly from organics. However, our rare finds (only two grains so far) with clearly recognizable relics of framboidal pyrite (Fig. 4 j, k) suggest instead that at least part of the post-organics diamond paramorphs were formed after

partially destroyed organics, perhaps in the form of lignin, which is able to preserve relics of the initial organics morphology within sedimentary rocks.

Additionally we have to discuss about the poorly ordered diamond and carbon matrix within the after-organic diamond paramorphs. According to the UV Raman spectra (Fig. 6, spectra 3, 4; Fig. 7) the diamond band 1317–1326 cm^{-1} is observed with a significant downshift from the standard T_{2g} mode of cubic diamond. Many scientists ascribe such a shift to lonsdaleite (*e.g.* Smith & Godard, 2009, 2013; Karczemska, 2010; Goryainov et al., 2014; Jones et al., 2016). However, the downshift can be explained in first place by the nanocrystalline nature of the impact diamonds (Ferrari, 2004; May et al., 2008; Osswald et al., 2009; Vul`, 2006; Yoshikawa et al., 1993, 1995). In many studies explaining the downshift by the presence of lonsdaleite (*e.g.* Smith & Godard, 2009, 2013), the used laser excitation was quite high, which has to result in essential overheating (May et al., 2008; Isaenko & Shumilova, 2009; Shumilova et al., 2014), with a large red-shift of the diamond line. At the same time, the nanocrystalline nature of the impact diamond studied by Smith & Godard (2009), as shown by the large FWHM (54–96 cm^{-1}) in the Raman spectra, can provide a diamond-line downshift explained by a phonon confinement effect (Yoshikawa et al., 1993, 1995; Osswald et al., 2009). Thus, considering the various possible reasons for the Raman diamond-line downshift, the presence of lonsdaleite cannot be established on this simple basis but requires independent additional high-resolution studies. In many published cases the lonsdaleite presence is not evidently proven.

In our case, on the basis of X-ray diffraction, electron diffraction and AFM observations, we did not recognize either lonsdaleite or any texture like in after-graphite impact diamonds (Kvasnytsya & Wirth, 2013; Masaitis et al., 1998). Thus, we conclude that the large Raman diamond-line downshift in after-organic diamond paramorphs is due to their nanocrystalline structure. Yezersky (1986) mentioned rare particles with texture and the very rare presence of lonsdaleite among after-coal diamonds, but without detailed description, so that it is not possible to ascertain their correctness.

In the UV Raman spectra of after-organic diamond paramorphs (Fig. 6, spectra 3, 4), the wide band centered at 1225–1260 cm^{-1} is assigned as a red-side shoulder of the certainly narrower diamond band at 1317–1326 cm^{-1}. This shoulder cannot be a D band of graphitic carbon as it must not be present for the used UV laser excitation (Ferrari, 2004). According to previous studies (Yoshikawa et al., 1993, 1995; Prawer, 2000; Osswald et al., 2003; Ferrari, 2004; Piscanec et al., 2005; Vul`, 2006), this shoulder band belongs to nanocrystalline diamond with crystallite sizes of about several nanometers (sub-nanocrystalline diamond) and smaller – up to amorphous tetrahedral diamond-like carbon (ta-C) with some presence of amorphous sp^2 carbon at the nanocrystallite boundaries, as indicated in the UV Raman spectra by a wide G band (1600–1650 cm^{-1}). The sub-nanocrystalline diamond, ta-C and amorphous sp^2 carbon, in some cases, are probably accompanied by a C=O band (about 1730 cm^{-1}).

It is interesting that similar Raman features have been described for meteoritic nanodiamonds from Efremovka (CV3) and Orgueil (CI) chondrites (Shiryaev et al., 2011) and synthetic detonated nanodiamonds (Vul`, 2006).

6.3. Proposed mechanism of after-coal diamond formation

Analysis of after-coal diamonds features clearly shows essential difference from after-graphitic impact diamonds: specific morphology of rounded grains and post-organic paramorphs; porous micro- and nano-structure; the absence of texture and the presence of well-formed octahedral diamond nanocrystals of the polycrystalline grains.

Based on the features of the initial carbonaceous matter and the established typomorphic features of after-coal diamond, we propose a formation mechanism alternative to the well-known direct graphite-diamond transition (diffusion-less) (*e.g.* Lonsdale, 1971; Kurdumov et al., 2012; Xie et al., 2014) and to the poorly known diffusion-limited reconstructive mechanism (Borimchuck et al., 1991).

According to Yezerskiy (1986) the initial coals of the Kara target include 1.42–2.73 % of hydrogen and 0.8–1.49 % of nitrogen (oxygen content was not measured, but can reach several

547 percent for the relevant coal stages – from bituminous to anthracite). Thus, diamond formation
548 from the coal precursor implies first of all the carbonization of the coal matter. The few studies
549 available on transformations of coal and organic compounds under shock pressure (~~Tyburczy et~~
550 ~~al., 1986~~; Borimchuck et al., 1991; Peterson et al., 1997; Kurdyumov et al., 2009; Korochantsev,
551 2012) allow one to predict possible transformations. According to shock high temperatures of
552 large impacts (*e.g*. Masaitis et al., 1998; Langenhorst, 2002) and published experiments
553 (Korochantsev, 2012), we suppose a high-temperature pyrolysis as the initial stage of coal
554 transformation, with destruction of long-range organic compounds (preferably of aliphatic
555 varieties), resulting in fluid phase removal (as supported by observed pores within diamond
556 aggregates) and formation of amorphous pure carbon and soot (Borimchuk et al., 1991;
557 Kurdyumov et al., 2009). The high shock temperatures up to 4000 K (Schmitt et al., 2005;
558 Kurdyumov et al., 2012, 2013) can allow some short-distance diffusion of amorphous carbon,
559 similar to experimentally produced process (Borimchuk et al., 1997; Kurdyumov et al., 2013)
560 with fast diamond/graphite crystallization to idiomorphic lonsdaleite-free/texture-free
561 nanocrystallites and carbon polymerization at quenching to glass-like carbon, as analysed in the
562 impact products by Raman spectroscopy and TEM.

563 **6.4. Implications: relation to carbonado**

564 According to our data and Yezerskiy`s study (1986), the after-coal diamonds from the Kara
565 astrobleme are quite similar to carbonado, including a light isotopic carbon composition, a
566 lonsdaleite-free, texture-free and porous structure, lack of crystallites of preferred orientation,
567 presence of well-shaped crystallites, and blue luminescence. After-coal diamonds are therefore a
568 strong piece of evidence in support of the impact hypothesis for the origin of carbonado, whose
569 nature has been debated for decades (*e.g*. Kaminsky, 1979; 1987, 1991; Smith & Dawson, 1985;
570 Yezerskiy, 1986; DeCarli 1987; Galimov et al., 1987; Heaney et al., 2005; Kagi et al., 2007;
571 Rondeau et al., 2008; Petrovsky et al., 2010; Piazolo et al., 2016). Some difference in mineral
572 inclusions and elemental impurities in known carbonados could be a result of different target in

different parts of the Earth's crust. A detailed comparison between after-coal diamond and carbonado is scope for future work.

7. CONCLUSION

On the basis of the provided complex study we have corrected understanding of carbon phases within Kara astrobleme impact products presented by glass-like carbon, graphite and 2 types of after-coal diamonds – sugar-like (with 2 subvarieties) and after-organics paramorphs. The tight growths of diamond with glass-like carbon are quite often, where the latter forms covering of a diamond core.

The novel afetr-organic diamond paramorphs have been found for the first time and described in detail. This type of impact diamond is widely spread through the Kara impact rocks locally bringing the huge concentrations up to first thousand carat per ton.

Our results demonstrate for the first time the nanostructural features of after-coal impact diamonds describing their enigmatic character, which is quite different from well-studied and widely known after-graphitic impact diamonds by idiomorphic nanocrystallites within diamond aggregates, presence of rounded shapes and after-organics morphology with nice preserved nanorelief, texture and lonsdaleite absence, porous micro- and nanostructure, presence of some sub-nanocrystalline–ta-C carbon matrix. The lack of lonsdaleite is one of the most important typomorphic feature of the after-coal impact diamonds, which in a complex of the other listed features makes them similar to carbonado. Thus, future detail comparison of after-coal impact diamonds and carbonado can help understand the latter secret.

The observations support probability of at least two stages of diamond formation through pyrolysis and subsequent diffusion-limited reconstructive mechanism of carbon.

The Kara impact object can be a basis for fundamental studies of after-coal impact diamond which may even be more widely spread through the Earth than after-graphitic ones. Thus, the presented data can be used for searching for new prospective astroblemes with huge

599 diamond resources at large impact craters around the world where some coal, peats or even just
600 living organics are present in the target matter.
601
602 **ACKNOWLEDGEMENTS**
603 The authors greatly thank Dr. V.L. Masaitis and Dr. M.S. Machshak for help and fruitful
604 discussions; Dr. A.V. Zuravlev for scientific consultation; Prof. J. Jaszczak for help in English
605 editing; A.E. Shmyrov for help in field and samples preparation; S.S. Shevchuk for help in SEM
606 studies; V.A. Radaev for AFM observations and statistical measurements; E.V. Sysol, G.N.
607 Panfilova, M.Yu. Sokerin for technical assistance. Also we greatly thank Prof. Dr. F.V.
608 Kaminsky and an anonymous reviewer for the detailed manuscript analysis and advices that
609 improved the paper. The study of the diamond-bearing impact melt rocks, impact glasses and
610 suevite varieties was funded by the Russian Science Foundation (Project # 17-17-01080), the
611 study of impact diamonds was provided through the Russian Foundation for Basic Research
612 (RFBR project #17-05-00516).
613
614 **REFERENCES**
615
616 Borimchuk N.I., Zelyavskiy V.B., Kurdyumov A.V., Ostrovskaya N.F., Trefilov V.I.,
617 Yarosh V.V. (1991) Mechanism of direct phase transformations of soot and coal to diamond
618 under impact pressing. Doklady Academy of Sciences, 321, 1, 95–98 (in Russian).
619 Bundy, F.P, Kasper, J.S. (1967): Hexagonal diamond – a new form of carbon. Journal of
620 Chemical Physics, 46, 3437–3446.
621 Bundy F.P., Basset W.A., Weathers M.S., Hemley R.J., Mao H.K., Goncharov A.F.
622 (1996): The pressure-temperature phase and transformation diagram for carbon: updated through
623 1994. Carbon, 34, 141–153.

624 DeCarli, P.S. (1995): Shock wave synthesis of diamond and other phases. in “Material
625 Research Society symposium” Proceedings, 383, 21–31. DeCarli, P. S. (1998): More on the
626 possibility of impact origin of carbonado. AIP Conf. Proc. 429, 681. http://dx.doi.org.sci-
627 hub.cc/10.1063/1.55580.El Goresy, A., Gillet, P., Chen, M., Kunstler, F., Graup, G., Stahle, V.
628 (2001): In situ discovery of shock-induced graphite-diamond transition in gneisses from the Ries
629 crater, Germany. American Mineralogist, 86, 611–621.
630 El Goresy, A., Dubrovinsky, L.S., Gillet, Ph., Mostefaoui, S., Graup, G., Drakopoulos, M.,
631 Simionovici, A. S., Swamy, V., Masaitis, V.L. (2003): A novel cubic, transparent and superhard
632 polymorph of carbon from the Ries and Popigai craters: implications to understanding dynamic-
633 induced natural high-pressure phase transitions in the carbon system. in: Abstracts of Lunar and
634 Planetary Science XXXIV, 1016.
635 Ferrari, A. C. & Robertson, J. (2004): Raman spectroscopy of amorphous, nanostructured,
636 diamond-like carbon, and nanodiamond. Phil. Trans. R. Soc. Lond. A., 362, pp 2477–2512.
637 Galimov, E.M., Kaminskiy, F.V., Kodina, L.A. (1985): New data on carbonado carbon
638 isotope compositions. Geochem. Int., 22, 18–21.
639 Goryainov S.V., Likhacheva A.Y., Rashchenko S.V., Shubin A.S. Afanas`ev V.P.,
640 Pokhilenko N.P. (2014): Raman identification of lonsdaleite in Popigai impactites. J. Raman
641 Spectrosc. 2014, 45, 305–313.
642 Heaney, P. J.; Vicenzi, E. P.; De, S. (2005): Strange Diamonds: the Mysterious Origins of
643 Carbonado and Framesite. Elements. 1 (2): 85. doi:10.2113/gselements.1.2.85.
644 Harris P.J.F. (1997) Structure of non-graphitising carbons. International Materials
645 Reviews, 42(5), 206–218.
646 Ievlev, A.A. and Belyaev, A.A. (1990): Electron microscopic and microdiffraction study of
647 organic matter of black shales of Pay-Khoy. Oil Shales, 7(1), 42–46 (in Russian).
648 Isaenko, S.I. & Shumilova, T.G. (2011): Thermostimulated splitting of Raman active
649 lonsdaleite modes. Vestnik of the Institute of Geology Komi SC UB RAS, 9, 29–33 (in Russian).

Kagi, H., Sato, S., Akagi, T., and Kanda, H., 2007 (2007): Generation history of carbonado inferred from photoluminescence spectra, cathodoluminescence imaging, and carbon-isotopic composition. American Mineralogist. 92: 217–224. doi:10.2138/am.2007.1957.

Kaminsky, F.V. (1987): Genesis of polycrystalline carbonado diamond aggregates. Dokl. Akad. Nauk SSSR Earth Sci. Section, 291, 439-440.

Kaminsky F.V. (1991) Carbonado and yakutite: properties and possible genesis. Proceedings of the Fifth International Kimberlite Conference, V.2. Diamonds: Characterization, genesis and exploration. Ed.: H.O.A. Meyer & O.H. Leonardos. Published by Companhia de Pesquisa de Reeursos Minerais – CPRM, Rio de Janeiro, RJ – Brasil. p. 136–143.

Kaminsky, F.V., Kirikilitsa, S.I., Yeryomenko, G.K., Polkanov, Yu.A., Khrenov, A.Ya. (1979) New data on Brazilian carbonado. Doklady AN SSSR, 249, 443–445 (in Russian).

Karczemska A.T. (2010) Diamonds in meteorites – Raman mapping and cathodoluminescence studies. Journal of Achievements in Materials and Manufacturing Engineering, 43(1), 94–107.

Kis, V.K., Shumilova, T., Masaitis, V. (2016): HRTEM study of Popigai impact diamond: heterogeneous diamond nanostructures in native amorphous carbon matrix. Phys. Chem. Minerals, DOI 10.1007/s00269-016-0825-6.

Koeberl, C., Sharpton, V.L., Murali, A.V., Burke, K. (1990) Kara and Ust-Kara impact structures (USSR) and their relevance to the K/T boundary event. Geology, 18, 50–53.

Kolesnikov, E. M., Nazarov, M.A., Badjukov, D.D., Lebedeva, L.M., Myasnikova,V.L. (1990) Current results of potassium-argon dating of the Kara impact structure. Lunar and Planetary Science XXI, 649–650.

Kolesov, B.A. (2009) Raman spectroscopy in inorganic chemistry and mineralogy. Novosibirsk, UB RAS Press, 189 p. (in Russian).

Korochantsev, A.V. (2004) Shock transformation of bitumens: application to organic matter of meteorites and impactites. PhD thesis report, Moscow. 27 p. (in Russian)

Kurdyumov A.V., Britun V.F., Yarosh V.V., Borimchuk N.I., Danilenko A.B., Zelyavskiy V.B. (2009) Phase transformations of soot under high temperature impact pressing. J.Superhard materials, 5, 36–43 (in Russian).

Kurdyumov, A.V., Britun, V.F., Yarosh, V.V., Danilenko, A.I., Zelyavskii, V.B. (2012) The influence of the shock compression conditions on the graphite transformations into lonsdaleite and diamond. J. Superhard Mater., 34(1), 19–27.

Kvasnytsya, V. & Wirth, R. (2013): Micromorphology and internal structure of apographitic impact diamonds: SEM and TEM study. Diamond & Related Materials, 32, 7-16.

Langenhorst, F. (2002): Shock metamorphism of some minerals: Basic introduction and microstructural observations. Bulletin of the Czech Geological Survey, 77, 265–282.

Langenhorst, F., Shafranovsky, G., Masaitis, V.L. (1998): A comparative study of impact diamonds from the Popigai, Ries, Sudbury, and Lappajarvi craters. Meteoritics & Planetary Science, 33 (4), A90–A91.

Lonsdale, K. (1971): Formation of lonsdaleite from single-crystal graphite. Am. Mineralogist, 56, 333–336.

Lutoev, V.P., Lysyuk, A.Yu. (2015): Structure and texture of silica of the Kara astrobleme impactites. Vestnik IG Komi SC UB RAS, 9, 24–32 (in Russian).

Mal`kov, B.A., Andreichev, B.L. (2010): Diamond-bearing tagamites of Kara astrobleme. Vestnik IG Komi SC UB RAS, 3(183) (in Russian).

Martirosyan, O.V. (2014) Factors and mechanisms of structural evolution of organic mineraloids. Doctoral thesis. Syktyvkar. 38 p. (in Russian).

Masaitis, V. L. (1975) Astroblemes in the USSR. International Geology Review, 18, 1249–1258.

Masaitis, V.L., Futergendler, S.I., Gnevushev, M.A. (1972): Diamonds in impactites of the Popigai meteoritic crater. Zapiski Vsesoyuznogo Mineralogicheskogo Obshestva, 101 (1), 108–112 (in Russian).

Masaitis, V.L., Shafranovsky, G.I., Yezersky, V.N., Reshetnyak, N.B. (1990): Impact diamonds in ureilites and impactites. Meteoritika, 49, 180–196 (in Russian).

Masaitis, V.L., Shafranovsky, G.I., Grieve, R.A.F., Langenhorst, F., Peredery, W.V., Therriault, A.M., Balmasov, E.L., Fedorova, I.G. (1999): Impact Diamonds in the Suevitic Breccias of the Black Member of the Onaping Formation, Sudbury Structure, Ontario, Canada. Geological Society of America, Special Paper, 339, 317–321. Mashchak, M.S. (1990) Geological environment of impact craters formation in Pay-Khoy. In: Impact craters at Mesozoic and Cenozoic boundary. Ed. V.L. Masaitis. Leningrad, Science. p. 24–37 (in Russian).

Mashchak, M. S. (1991) Morphology and structure of the Kara and Ust'-Kara astroblemes. International Geology Review, 33:5, 433-447, DOI: 10.1080/00206819109465701.

May, P.V., Overton, Ph., Smith, J.A., Rosser, K.N. (2008) Multi-wavelength Raman Spectroscopy of Nanodiamond Particles. Mater. Res. Soc. Symp. Proc., 1039, 1039-P15-03.

Nazarov, M. A., Badjukov, D. D., Alekseev, A. S. (1989) Morphology of the Kara and Ust'Kara impact craters, USSR. Lunar and Planetary Science XX, 762–763.

Nazarov, M. A., Badjukov, D. D., Kolesnokov, E. M., Barsukova, L. D., Kolesov, G. M. (1989) Geology, geochemistry and geochronology of the Kara impact structure. Meteoritics, 24, 307–308.

Nazarov, M. A., Badjukov, D. D., Barsukova, L. D., Alekseev, A. S. (1991) Reconstruction of original morphology of the Kara impact structure and its relevance to the K/T boundary event. Lunar and Planetary Science XXII, 959–960.

Nazarov, M. A., Badjukov, D. D., Alekseev, A. S. (1992) The Kara structure as a possible K/T impact site. Lunar and Planetary Science XXIII, 969–970.Ohfuji, H., Irifune, T., Litasov, K.D., Yamashita, T., Isobe, F., Afanasiev, V.P., Pokhilenko, N.P. (2015): Natural occurrence of pure nanopolycrystalline diamond from impact crater. Scientific Reports | 5:14702 | DOI: 10.1038/srep14702.

Osswald S., Mochalin V.N., Havel M., Yushin G., Gogotsi Y. (2009) Physical Review B 80, 075419 (2009) Phonon confinement effects in the Raman spectrum of nanodiamond. Physical Review B 80, 075419(9).

Peterson, E., Horz, F., and Chang, S. (1997) Modification of amino acids at shock pressures of 3.5 to 32 GPa. Geochim. Cosmochim. Acta 61:3937–3950.

Petrovsky, V. A., Shiryaev, A. A., Lyutoev V. P., Sukharev, A. E., Martins, M. (2010) Morphology and defects of diamond grains in carbonado: clues to carbonado genesis, Eur. J. Mineral., 22, 35-47.

Piazolo, S., Kaminsky, F.V., Trimby, P., Evans, L. Luzin V. (2016) Carbonado revisited: Insights from Neutron diffraction, high resolution, orientation mapping and numerical simulations. Lithos, DOI: 10.1016/j.lithos.2016.09.011.

Piscanec, S., Mauri, F., Ferrari, A.C., Lazzeri, M., Robertson, J. (2005): Ab initio resonant Raman spectra of diamond-like carbons. Diamond & Related Materials, 14, 1078– 1083.

Prawer, S., Nugent, K.W., Jamieson, D.N., Orwa, J.O., Bursill, L.A., Peng, J.L. (2000): The Raman spectrum of nanocrystalline diamond. Chemical Physics Letters, 332, 93–97.

Reshetnyak, N.B., Yezerskiy, V.A. (1990) Combination scattering spectroscopy of natural diamonds. Mineralogical Journal, 12(5), pp. 3–9 (in Russian).

Rondeau, B., Sautter, V., Barjon, J. (2008): New columnar texture of carbonado: Cathodoluminescence study. Diamond and Related Materials. 17 (11), 1987. doi:10.1016/j.diamond.2008.04.006.

Schmitt, R.T., Larke, C., Lingemann, C.M., Siebenschock, M., Stoffer, D. (2005) Distribution and origin of impact diamonds in the Ries crater, Germany. *in* ‘‘Large meteorite impacts III’’, Th. Kenkmann, F. Horz, A., ed. Deutsch. ~~p. cm.~~, Geol. Soc. Amer. Spec. Paper 384, 299–314.

751 Selivanovskaya, T.V., Maschak, M.S., Masaitis, V.L. (1990): Impact breccia and
752 impactites of Kara and Ust`-Kara astroblemes. In: Impact craters at Mesozoic and Cenozoic
753 boundary. Ed. V.L.Masaitis. Leningrad, Science, 1990. p. 55-96. (in Russian).
754 Shafranovsky, G.I. (1985): Crystallomorphology of paramorphs of diamonds after
755 graphite. Zapiski VMO, 114 (1), p. 30–34 (in Russian).
756 Shishkin, M.A., Shkarubo, S.I., Molchanova, E.B., Markina, N.B., Vanshtein, B.G. et al.
757 State Geological Map. Scale 1:1,000,000 (3rd edition). South-Karskaya series. R-41 – Amderma.
758 Report. Saint-Petersburg, VSEGEI, 2012. 383 p. (in Russian).
759 Shumilova, T., Kis, V., Masaitis, V., Isaenko, S., Makeev, B. (2014): Onion-like carbon in
760 impact diamonds from Popigai astrobleme. European Journal of Mineralogy, 26, 267–277.
761 Shiryaev A. A., Fisenko A. V., Vlasov I. I., Semjonova L. F., Nagel P., Schuppler S.
762 (2011) Spectroscopic study of impurities and associated defects in nanodiamonds from
763 Efremovka (CV3) and Orgueil (CI) meteorites. Geochimica et Cosmochimica Acta, 75, 3155–
764 3165.
765 Smith, J. V., Dawson, J. B. (1985): Carbonado: Diamond aggregates from early impacts of
766 crustal rocks? Geology, 13, 342–343.
767 Smith, D.C., Godard, G. (2009): UV and VIS Raman spectra of natural lonsdaleites:
768 Towards a recognised standard. Spectrochimica Acta - Part A: Molecular and Biomolecular
769 Spectroscopy, 73, 428–435.
770 Sokhor, M.I., Polkanov, Y.A., Yeremenko, G.K. (1973): A find of the hexagonal diamond
771 (lonsdaleite) in placers, USSR. Doklady Academy of Sciences USSR, 209, 118–121 (in
772 Russian).
773 Trieloff, M., Deutsch, A., Jessberger, E.K. (1998): The age of the Kara impact structure,
774 Russia. Meteoritics & Planetary Science, v. 33, pp. 361-372.
775 Udoratin, V.V., Konanova, N.V., Popov, I.V. (2010): Deep composition of Kara ring
776 structure. Proceedings of Komi SC UB RAS, 4, 47–51 (in Russian).

Val’ter, A.A., Eremenko, G.K., Kvasnitsa, V.N., Polkanov, Yu.A. (1992): Shock Metamorphogenic Carbon Minerals. Naukova Dumka, Kiev, 171 p. (in Russian).

Vishnevsky, S.A. (2007): Astroblemes. Novosibirsk, Nonparel`, 288 p. (in Russian).

Vul' A. Ya. (2006) Characterisation and physical properties of UNCD particles. In: Ultrananocrystalline Diamond (eds. O. Shenderova and D. Gruen). p. 379-404.

Xie, H., Yin, F., Yu, T., Wang, J.-T., Liang, C. (2014): Mechanism for direct graphite-to-diamond phase transition. Scientific Reports 4, Article number: 5930 doi:10.1038/srep05930.

Yezerskiy, V.A. (1982): Impactly metamorphosed coal substance in impactites. Meteoritika, 41: 134–140 (in Russian).

Yezerskiy V. A. (1986) High pressure polymorphs produced by the shock transformation of coals. International Geology Review, 28:2, 221-228. DOI:10.1080/00206818609466264.

Yudovich, Ya. E., Belyaev, A.A, Ketris, M.P. (1998) Geochemistry and ore genesis of black shales of Pay-Khoy. Saint-Petersburg: Science, 1998. 366 p. (in Russian).

Yushkin, N. P., Lysyuk, A. Yu. (2001) Scenarios and basic parameters of Kara impact event. Vestnik IG Komi SC UB RAS, 8, 14–17 (in Russian).

Figures

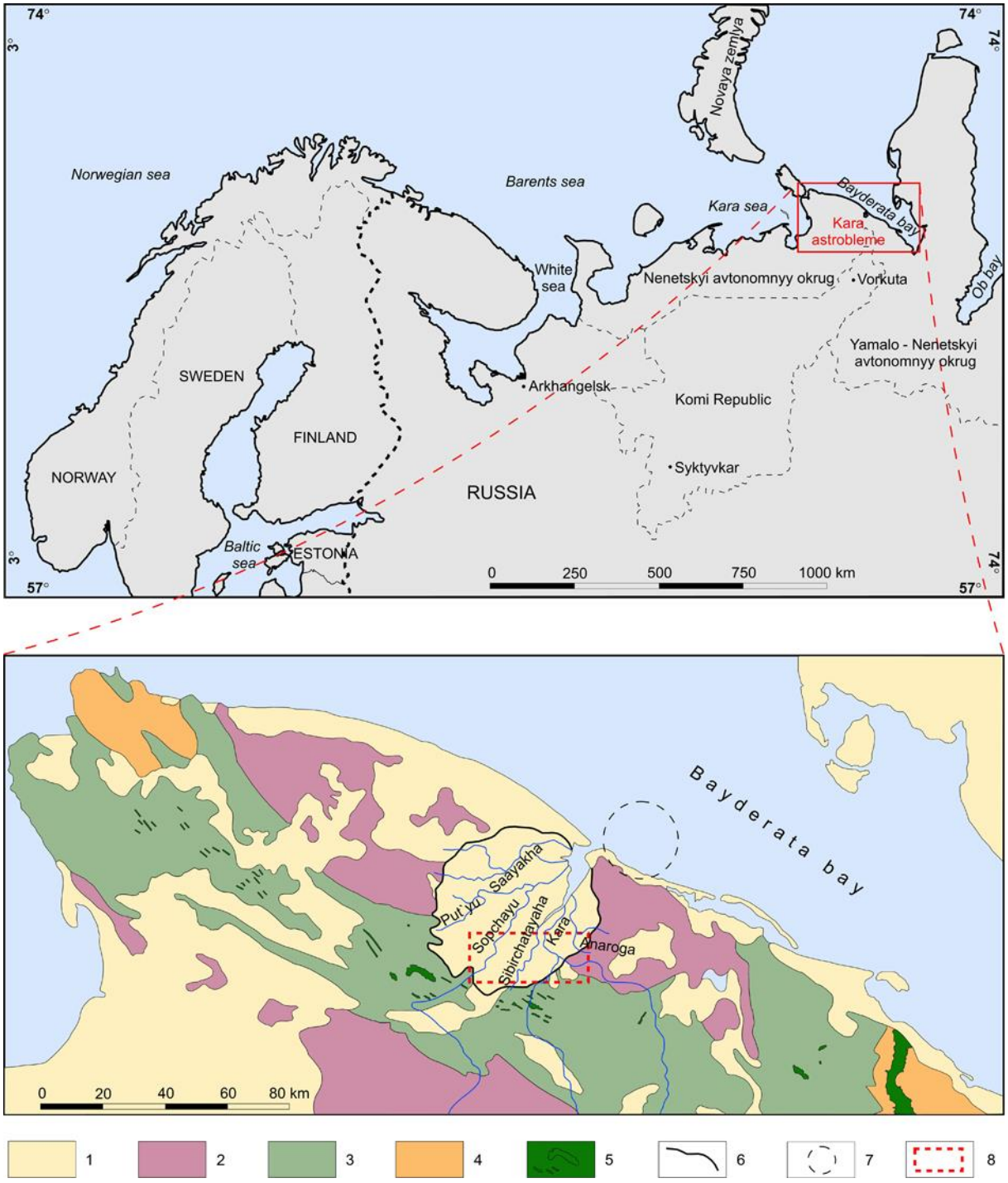

Fig. 1. Geological scheme of the Kara region territory modified after Yudovich et al. (1998) and Mashchak (1990) with additions: 1 - Pliocene-Quaternary sediments; 2 - Triassic and Permian deposits; 3 - Carboniferous, Devonian, Silurian and Ordovician sediments; 4 - Upper Proterozoic sediments; 5 - Late Devonian tabular body and dikes of dolerite and gabbro-dolerite; 6 - the border of the Kara astrobleme; 7 - the border of the Ust-Kara astrobleme; 8 - sampling region. Upset – geographic setting of the studied area. The color image is available within an on-line version.

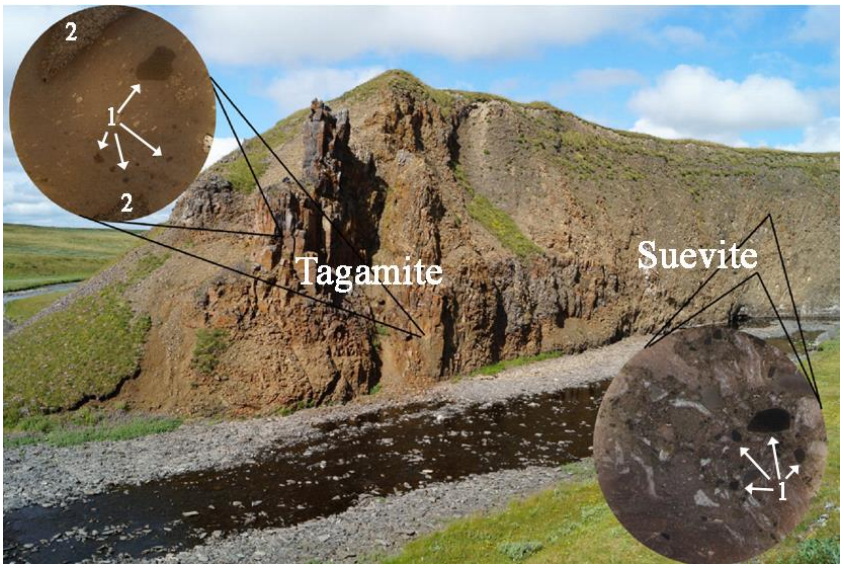

a

b

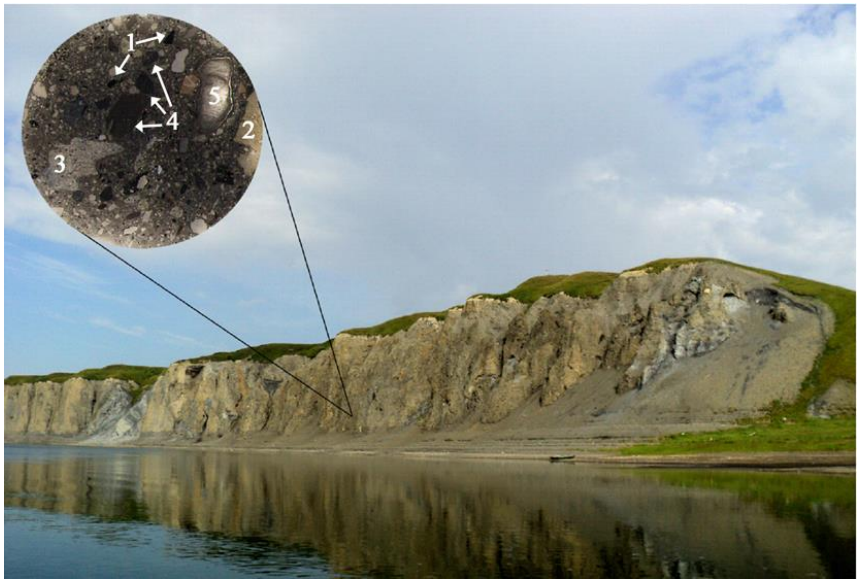

c

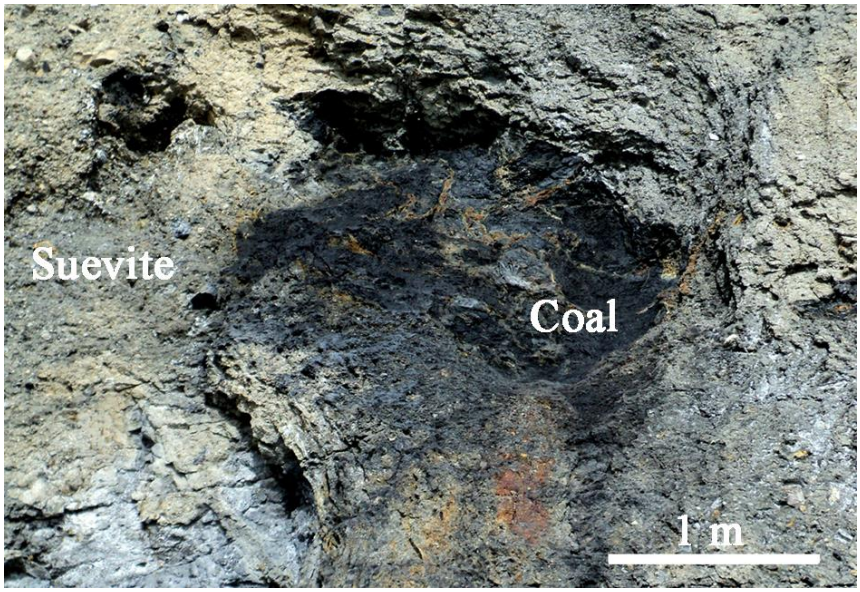

d

Fig. 2. Impactites of Kara astrobleme. a – tagamite (left inset) and co-following suevite after silicate rocks (right inset) from the outcrop maximum high of 20 m at the Anaroga River, b – 1x2 m coal fragment (dark grey, in a center) within the bottom part of the tagamite body, the Anaroga River. c – Suevite after organic-carbon-bearing carbonates and black shales, the visible outcrop length is about 700 m, at the Kara River; d – 1x2 m relict of a coal fragment (black, in the center) within suevite, from the right bank of the Kara River. Insets: 2a, c – thin polished sections (2 cm diameter) in transmitted light, numbers correspond to relict fragments: 1 – coal , 2

832 –sandstone, 3 – limestone, 4 – black shale; 5 – pore; 2b – coal pieces from a large coal fragment.

833 The color image is available within an on-line version.

834
835
836
837
838
839
840

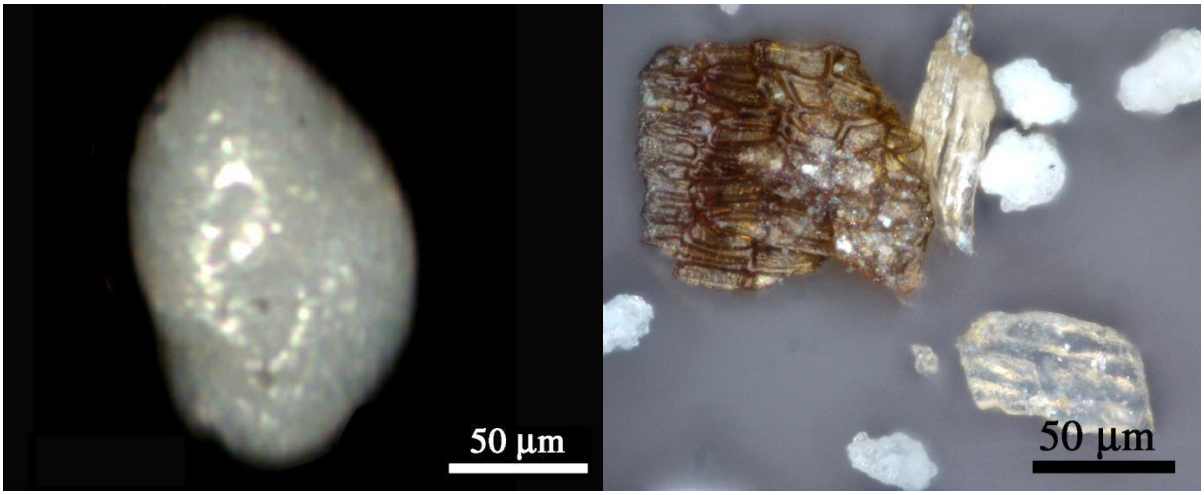

841

842 a b

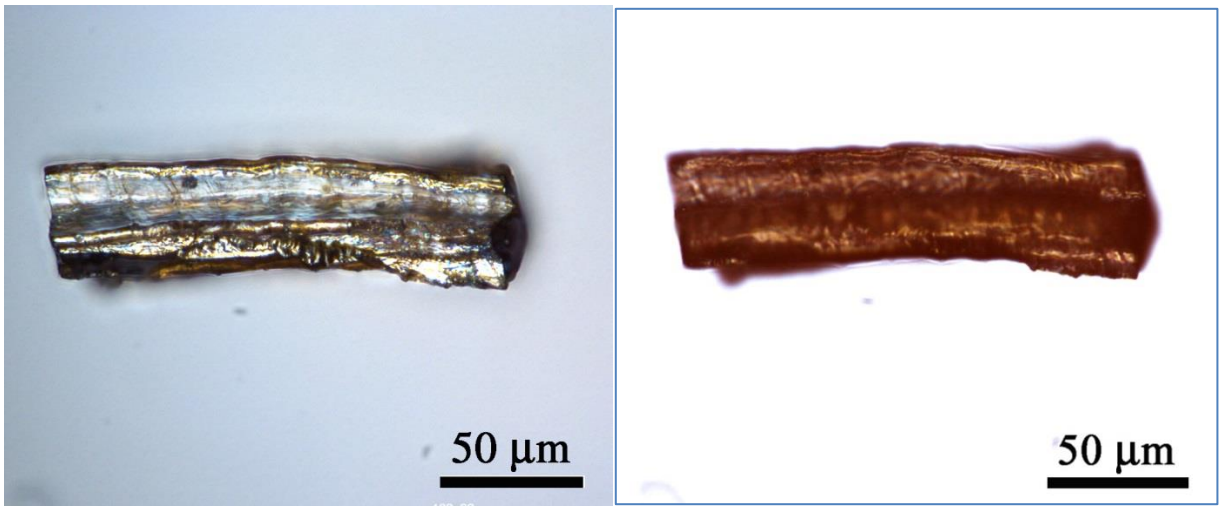

843

844 c d

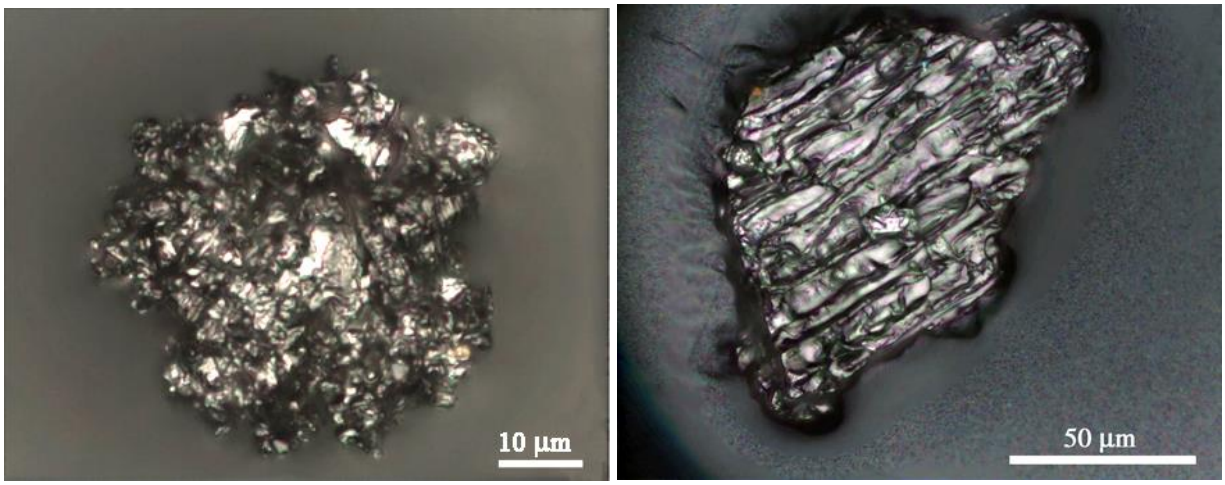

e f

Fig. 3. Optical images of the varieties of impact after-coal carbons obtained from thermochemical concentrate in unpolarized reflected light: a – Light gray, fully crystalline, dense sugar-like diamond with a rounded egg-like shape, in reflected light. A SEM image of the same grain is shown in fig. 4a; b – After-organic diamond paramorphs and friable sugar-like particles. A diamond paramorph after-organic relict (d – shown in transparent light); e – hedgehog-shaped graphite; f – GLC paramorph after organics. The color image is available within an on-line version.

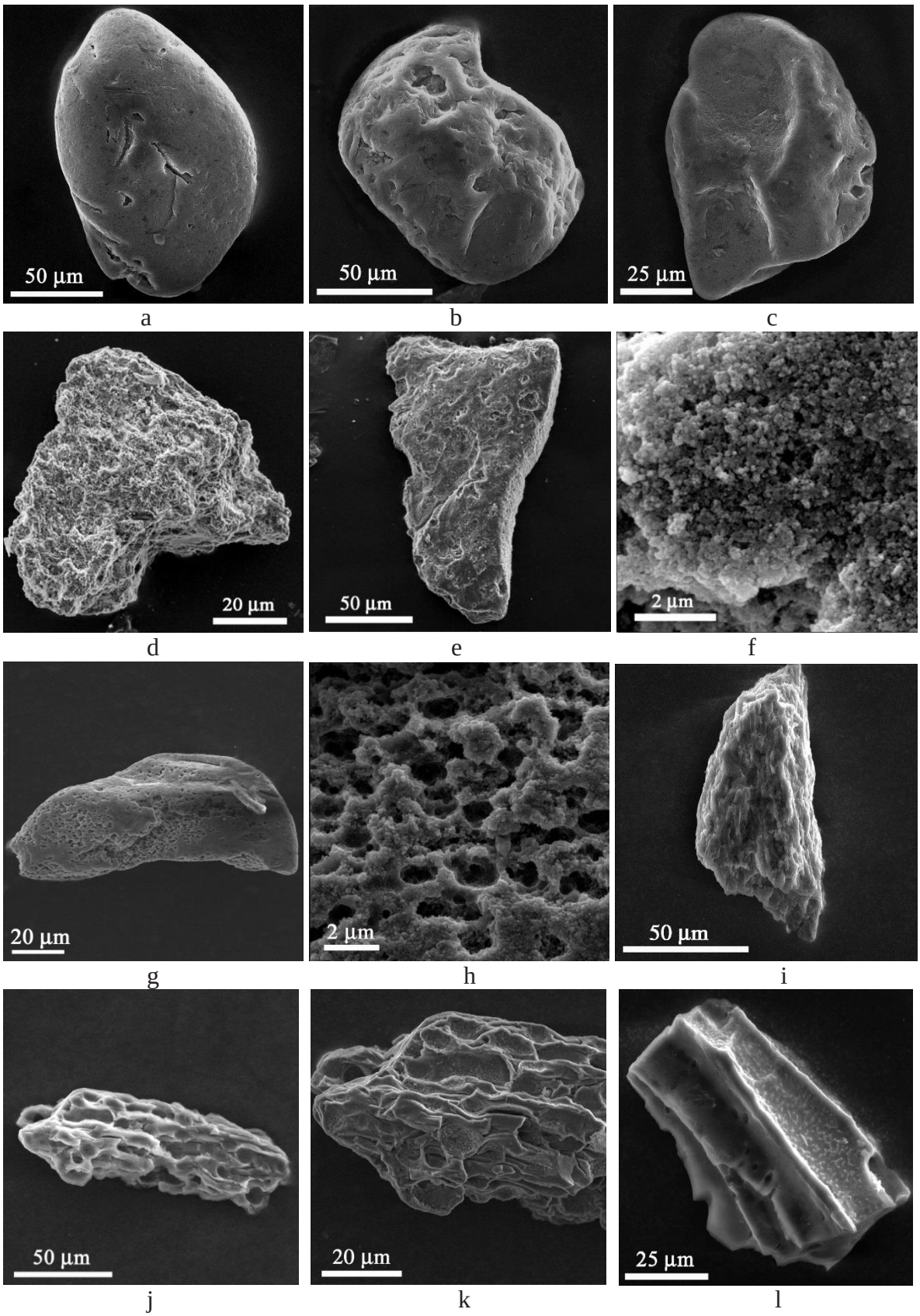

Fig. 4. SEM images of varieties of impact after-coal diamonds. a-f – Sugar-like diamonds. Dense rounded egg-like grain with deep cracks (a); dense rounded drop-like grains (b); dense irregular grain with rounded edges and smooth surface (c); white friable sugar-like particle (d);

white friable sugar-like particle (e) with a magnified fragment (f). Irregular sugar-like dense diamond with microporous structure (g) and a close-up (h). Brown poorly ordered after-organic diamond paramophs: i – diamond with fibrous morphology; j – After-organic paramorph with negative relict morphology after framboidal pyrite aggregates and close-up (k). l – Diamond paramorph with tiny relict organic morphology.

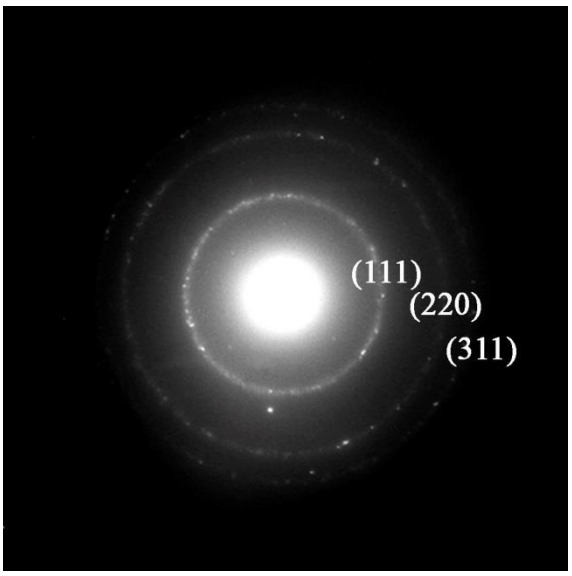

a

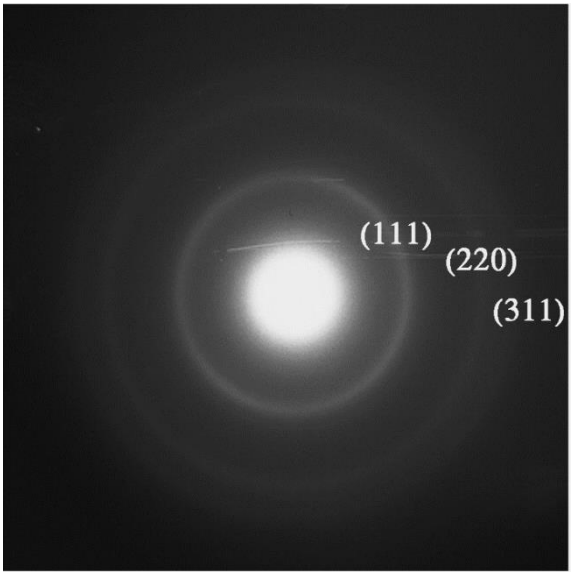

b

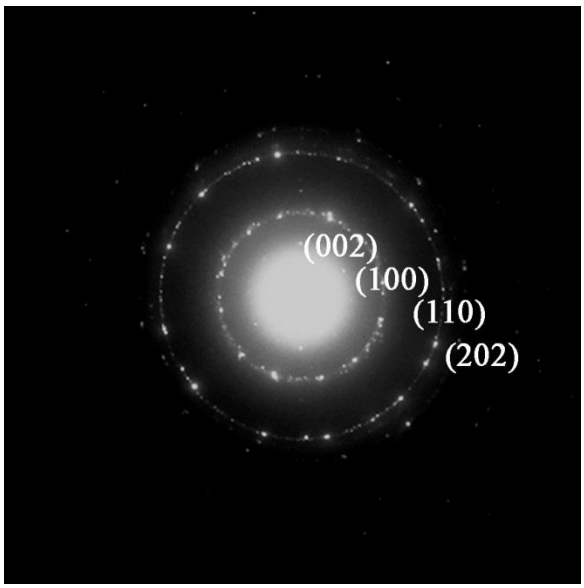

c

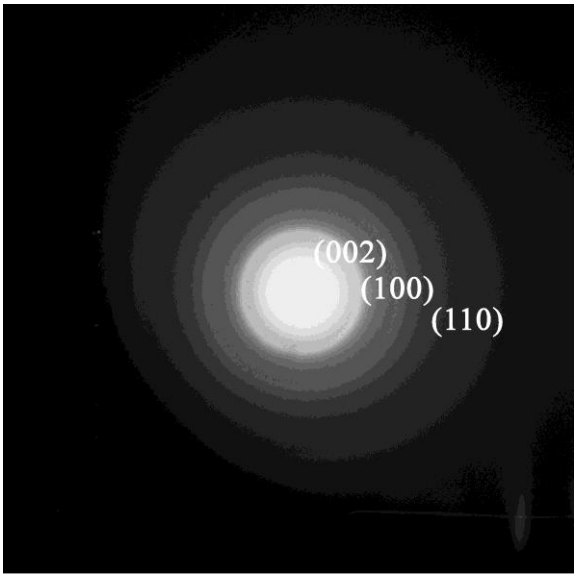

d

Fig. 5. Typical transmission electron microscopy data of Kara impact after-coal carbons, electron diffraction patterns: a – sugar-like diamond d_{111}= 2.06 Å, d_{220}= 1.27 Å, d_{311}= 1.07 Å; b – nanopolycrystalline diamond, d_{111}= 2.05 Å, d_{220}= 1.25 Å, d_{311}= 1.06 Å; c – polycrystalline graphite, d_{100}=2.11 Å, d_{110}=1.23 Å; d_{112}=1.155 Å; d – GLC, diffusion rings with maxima at d_{002}=3.38 Å, d_{100}=2.07 Å, d_{110}=1,23 Å. The phases identification has been supported by Raman spectroscopy measurements.

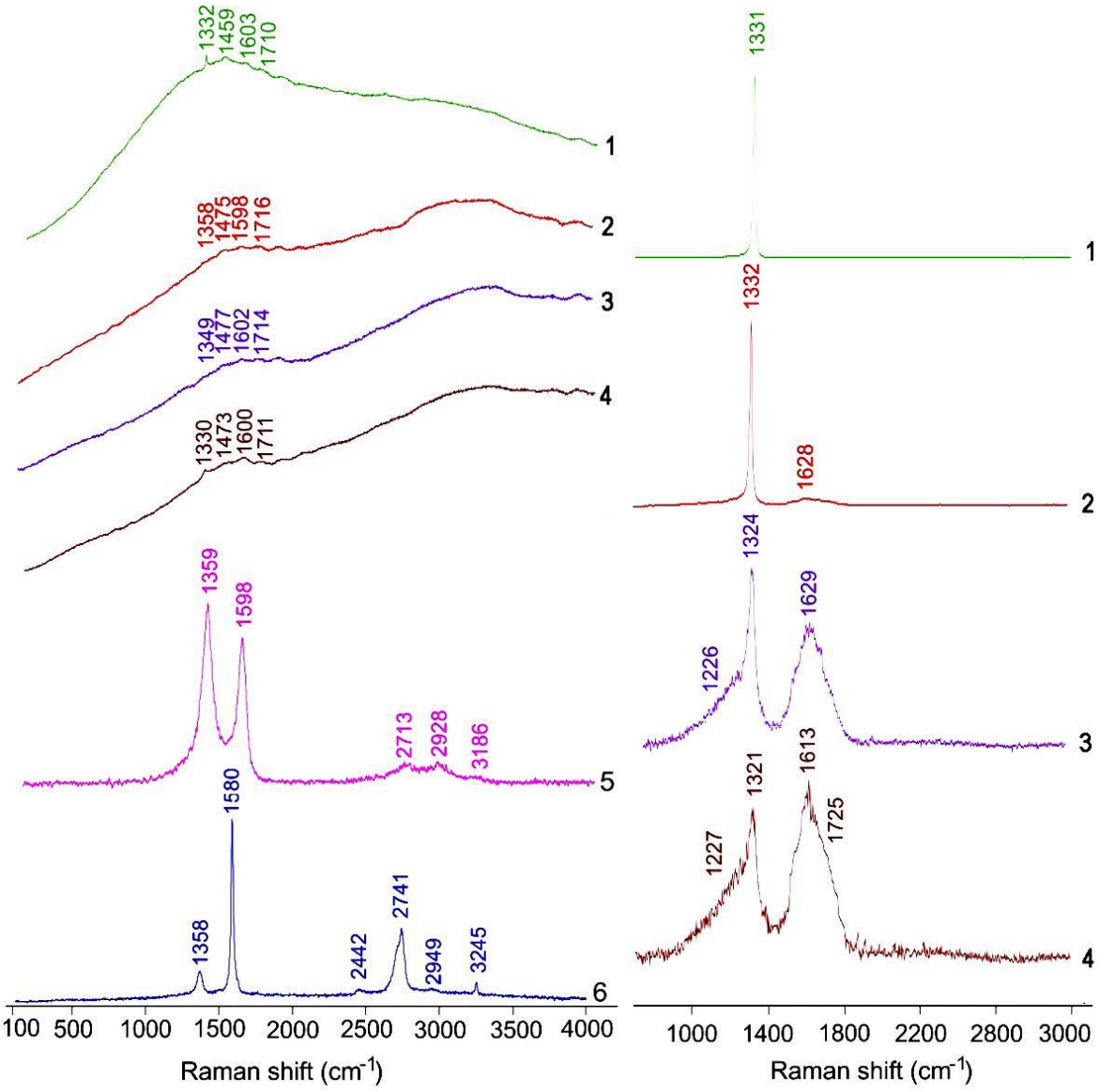

916

917

918 Fig. 6. Raman spectra for different impact after-coal carbons. Spectra on the left are for visible
919 laser excitation, and on the right for UV laser excitation. Spectra of micrograined sugar-like
920 well-ordered white diamonds: 1 – dense, 2 – friable. Spectra 3 and 4 are from less-ordered
921 brown diamonds, less ordered with different crystallinity, with 3 showing better crystallinity than
922 4. Spectrum 5 is from glass-like carbon. Spectrum 6 is from graphite. The color image is
923 available within an on-line version.

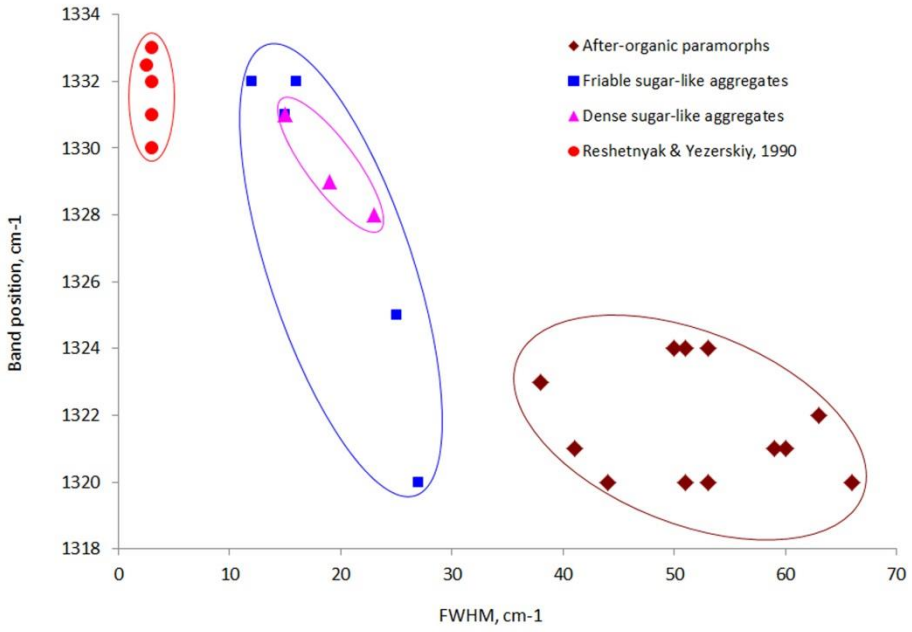

924

925 Fig. 7. Raman spectroscopy data of after-coal diamond varieties for A_{2g} diamond mode. The

926 color image is available within an on-line version.

927

928

929

930

931

932

933

934

935

936

937

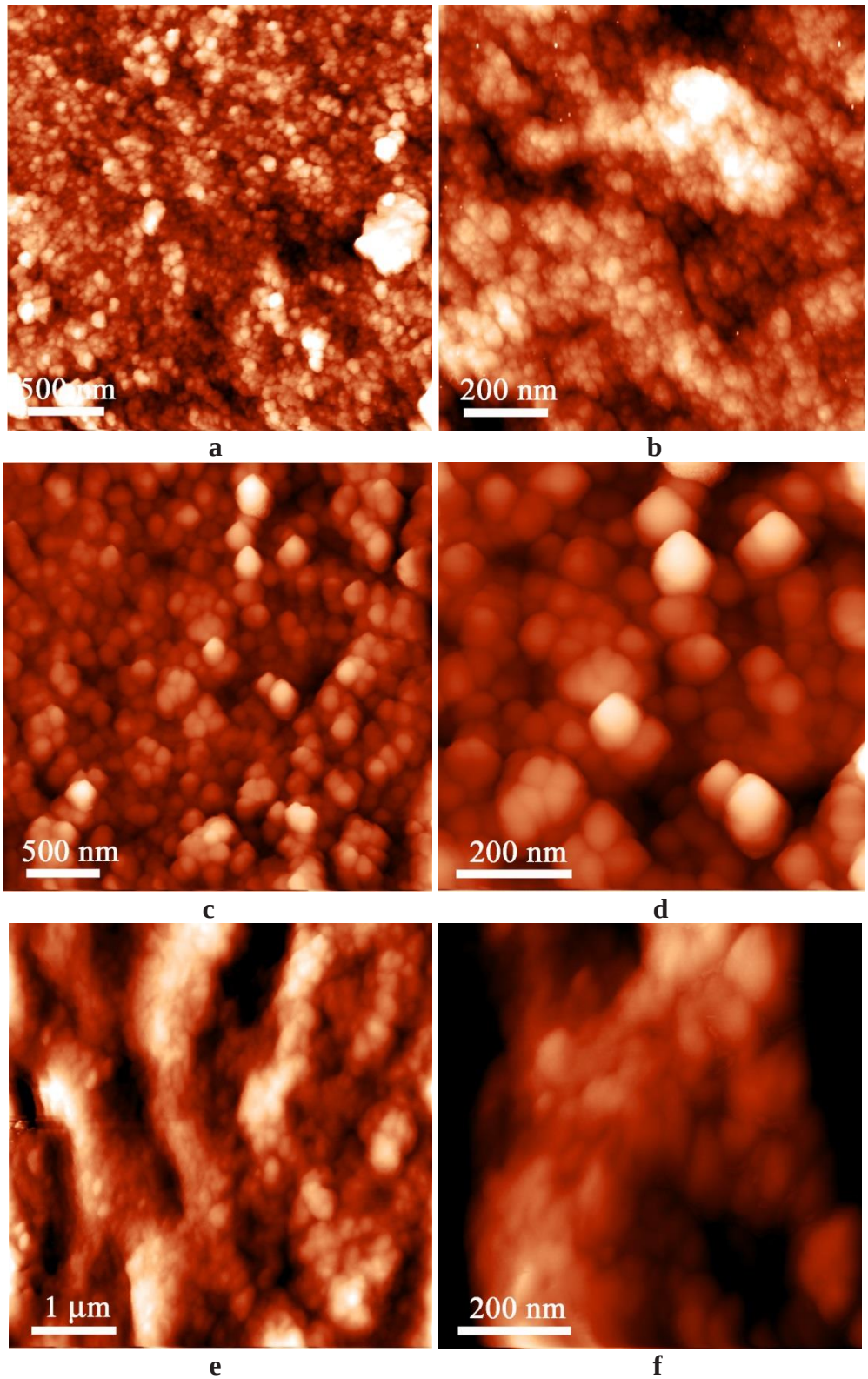

Fig. 8. Nano-scale features of after-coal impact diamonds by AFM data: a, b – White sugar-like dense diamond of irregular shape consisting of hierarchical diamond nanocrystal aggregates; c, d – Brown after-ogranic paramorph with fine-scale but well-defined octahedral nanocrystals; e, f – After-ogranic diamond paramorph with poorly recognizable nanocrystal morphology. The color image is available within an on-line version.

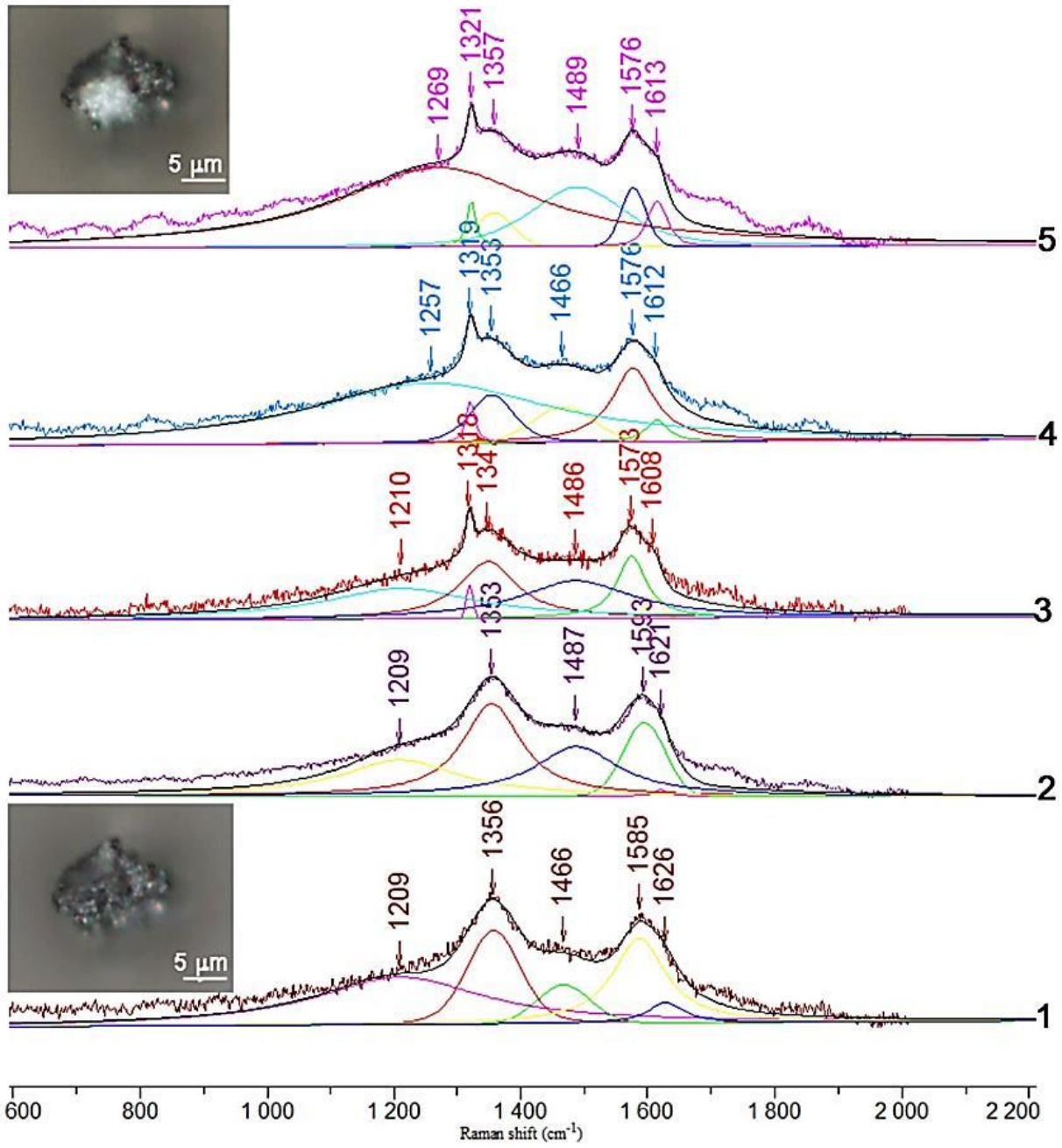

949

950 Fig. 9. Raman study of coated after-coal diamond using visible laser excitation (488 nm). 1-5
951 continually measured Raman spectra (1 - starting, 5 – final). Spectra 1 and 2 are at 1.2 mW laser
952 power, shown along with corresponding photo inset at the bottom. Spectra 3-5 are at 12 mW.
953 The corresponding upper photo inset reveals the recovered diamond as a bright central spot after
954 the 12 mW laser heating treatment. The colored curves are fitting of the spectra to components
955 with upper set band positions. The color image is available within an on-line version.

956